New dynamic multimode model for external cavity semiconductor lasers

A.J. Lowery, PhD

Indexing terms: Semiconductor lasers, Modelling

Abstract: A new, dynamic, time-domain, numerical model for external cavity lasers, based on the transmission-line laser model (TLLM), is introduced. This is able to show the evolution of spectra from large-signal modulated devices, even when the modulation pulsewidth is less than the external cavity round-trip delay. The model is demonstrated using short and long dispersionless cavities. Results in the time and spectral domains are in agreement with those of previous theoretical and experimental work.

1 Introduction

External cavity semiconductor lasers are constructed from two main components: a standard Fabry-Perot injection laser used as a gain block, and an external cavity coupled to one of the lasers facets acting as a passive resonator. The advantages of such an arrangement over a simple Fabry-Perot laser are that the static and dynamic linewidths are reduced [1]. The resonator has also been shown to increase the relaxation frequency of the laser under certain circumstances. This is usually equated to the upper limit of modulation frequency. Both narrow linewidths and high modulation frequencies are desirable for high-data-rate long-haul fibre-optic communication systems [2].

The external cavity is formed using a reflector placed up to several centimetres away from the rear facet of the laser. The front facet is used to couple power to a communications fibre, as shown in Fig. 1 [3–19]. The cavity will preferentially feed back optical power into the laser at a number of frequencies, depending on its phase length and coupling to the laser. If one of these frequencies lies close to a Fabry-Perot longitudinal mode and the material gain peak, and the feedback has the correct phase, the device will oscillate near to or at this frequency.

Unfortunately, especially for long cavities which are designed to give low linewidths, several cavity resonances may achieve the above lasing condition. In this case the laser will become multimoded. However, this problem may be solved by the inclusion of a dispersive filtering element into the cavity, as in Figs. 1*d–h* [12–19]. This work will concentrate on designs without a dispersive component [4–11]. However, it is easy to modify the proposed model to cover dispersive external cavities.

Paper 6709J (E13), first received 12th December 1988 and in revised form 17th April 1989

The author is with the Department of Electrical and Electronic Engineering, University of Nottingham, Nottingham NG7 2RD, United Kingdom

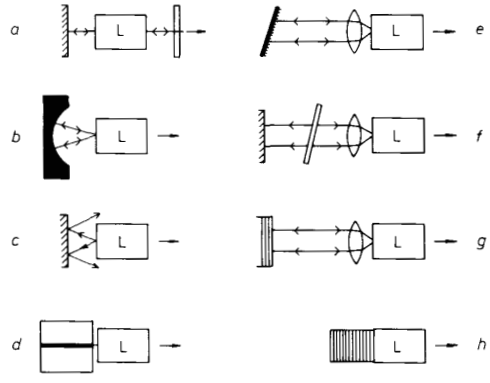

Fig. 1 *Some external cavity laser designs*
a Original gas-laser design proposed in Reference 3
b Hemispherical mirror [4, 5]
c Plane-mirror [6–9]
d Glass waveguide [10] or GRINrod [11]
e Grating [12–15]
f Etalon and plane mirror [16]
g Multilayer reflection filter [17]
h Distributed Bragg reflector [18, 19]
Designs (*e*)–(*h*) incorporate a dispersive (filtering) element and may use one anti-reflection coated facet

A long cavity will give a delay to the feedback pulse. This will have no consequence when the device is unmodulated (CW operation). However, if the device is to be modulated, the modulation rate will be limited because of this delay. An ideal model would show the effect of this delay.

One approach is to use the rate equations for carrier and photon density and to include a delayed term in the photon rate equation [1, 20]. The equations can then be solved numerically to obtain a large-signal temporal response [1]. However, it is difficult to include the effect of the feedback phase when using a rate equation for photon density. This phase will be shown to have an important bearing on the modulation characteristics of the device. It is also difficult to model more than a single wavelength. At best, a number of discrete wavelengths may be modelled using multiple rate equations for photon density.

Two assumptions have to be made when using a delayed term approach, namely that the photon and carrier concentrations within the laser cavity are in their steady-state profiles, and that multiple reflections within the external resonator are small. These become invalid when either very high speed modulation is used, or the external cavity has a high Q-factor. The problem of very high speed modulation may be solved by discretising the rate equations along the length of the cavity. Such a model has been used for laser amplifiers by Marcuse [21] and for cleaved coupled cavity (CCC) devices by Coldren

and Koch [22, 23]. Longitudinal discretisation is implicit in the proposed model, because sampling of the propagating waves in the time domain implies discretisation in the spatial domain. The effect of a high Q-factor in the external cavity is not implicit in the rate equation approach, but is a simplification to minimise storage requirements. This approximation need not be made with the present model, and has no bearing on the storage requirements.

Coldren's and Koch's model is especially interesting because it uses multiple rate equations to simulate the transition from multimode to single longitudinal mode (SLM) operation during a transient [23]. This transition is taken into account in the proposed model but with the advantage that the chirping of the individual modes is also modelled. This is because the variation of feedback phase is modelled over a large and continuous bandwidth.

One method of including feedback phase into a rate equation model is to use the photon field, rather than the photon density, as a variable. For example, Agrawal has derived four rate equations for the photon field and phase inside and outside the laser cavity [24]. When combined with a rate equation for carrier density, the device's modulation characteristics (FM and AM) can be found in the frequency domain. However, this model is limited to a single-longitudinal mode.

Another example, used in this paper, is to use rate equations for the left- and right-travelling fields, as proposed in Reference 25. Despite its title, this approach differs from that proposed here because it uses a single scattering matrix solved in the frequency domain rather than multiple scattering matrices solved in the time domain. It is therefore suited to steady-state problems.

Other field rate equation based models have been used to investigate the following external cavity laser characteristics: frequency and intensity instability [26], phase noise and modulation bandwidth [27], spectral behaviour [28], the relation between chirp and linewidth reduction [29, 30], and the production and propagation of chirped pulses through dispersive fibres [30]. This last application is interesting because the proposed model's output could be convoluted with the impulse response of a fibre to quantify the pulse dispersion.

This paper is concerned with the large-signal modulation and spectral characteristics of external cavity lasers with flat-frequency-response reflectors. The main assumption is that the delay within the external reflector is insignificant compared with the delay of the cavity, i.e. distributed Bragg reflector devices are excluded. However, unlike the above works, the delay of the external cavity can be larger than the modulation pulsewidth. This occurs when the cavity is longer than 3 cm at 8 Gbit/s.

2 Transmission-line laser model

The proposed model is an extended (sic) transmission-line laser model (TLLM). The TLLM is based on the transmission-line modelling (TLM) method for electromagnetic wave and diffusion problems, which was originally developed to characterise metallic waveguides [31]. The TLLM includes time-domain models for the spontaneous and stimulated emission processes, and was first applied to modulated semiconductor lasers by Lowery [32]. It has subsequently been used in the study of laser chirp [33], the study of multimode spectra [34], the prediction of laser amplifier bistability [35], the characterisation of laser amplifiers [36], the modelling of spontaneous emission damped relaxation oscillations [37], and the explanation of pulse compression in laser amplifiers [38]. A detailed introduction to this method is provided in [39].

The modelling method is especially suited to external cavity devices for two reasons. First, it models longitudinal variations in waveguide structure, optical field intensity, and emission mechanisms. Secondly, it models phase and amplitude over a wide and *continuous* bandwidth, essential for the study of frequency chirping and multimode spectra [33], and thirdly, the field quantities in the model have a one-to-one spatial correspondence to those in the real device. This correspondence provides easy modification and interpretation of the results.

Complex and inflexible mathematical treatments are avoided by the use of simple building blocks, each representing a longitudinal section of the cavity. Each block contains a scattering node which operates on samples of the forward- and backward-travelling waves. The nodes of adjacent blocks are connected using transmission-lines which delay the samples by exactly one iteration timestep, the timestep being linked to the node spacing by the velocity of light in the medium. This means that the samples need only be stored at the scattering nodes. At each iteration, the samples will be passed along the lines to adjacent nodes to be modified by their scattering matrices at the next iteration.

The scattering matrices represent the optical processes of stimulated emission, absorption and spontaneous emission. The models of processes can be made wavelength dependent using time-domain filters [32]. The amounts of stimulated and spontaneous emission are dependent on the average carrier concentration within the section. The carrier concentration is modelled using a numerically solved rate equation. This allows for nonlinear effects such as dynamic saturation of the cavity gain [35].

Earlier papers have provided the basic building blocks (and associated scattering matrices describing the nodes) for the cavity in a Fabry-Perot laser [32], the facets of a Fabry-Perot laser [33], a modified facet to allow external fields to be incident on laser amplifiers [35], and a modified cavity section including an improved spontaneous emission model [37]. This paper presents a block representing the delay of the external cavity and a scattering matrix to couple it to the Fabry-Perot model. When combined with the model including incident fields [35], a external cavity TLLM results.

In common with other TLLMs, the model assumes the following: a single transverse mode propagates, one polarisation is dominant, the current injection is uniform, the gain's wavelength dependence and the spontaneous emission spectral dependence (over a number of cavity resonances) can be represented by fixed Lorentzian functions, the spontaneous recombination lifetime is independent of carrier density, electron diffusion is negligible, and nonradiative recombination is negligible.

3 Model description and development

Many external cavity models use a wavelength-dependent effective reflectivity to describe the feedback. This technique could be used here by representing the frequency dependence using a time-domain filter. However, a much simpler method is to store the sampled outgoing wave from the laser cavity, and return it to the cavity after an appropriate delay and scaling. This

method has the advantage that the delay is modelled as well as the frequency dependence of the external cavity. It is also very simple to implement.

Multiple transits of the resonator, caused by reflections at the laser-chip/external-cavity interface, are dealt with by adding a fraction of the delayed signal to the new sample to be delayed. In this way, the external cavity behaves as a recursive filter. In formal terms, the laser-resonator interface can be described as a scattering matrix thus,

$$\begin{bmatrix} E_c^r \\ E_e^r \end{bmatrix} = \begin{bmatrix} S_{11} & S_{12} \\ S_{21} & S_{22} \end{bmatrix} \begin{bmatrix} E_c^i \\ E_e^i \end{bmatrix} \quad (1)$$

where E_c^i and E_e^i are the incident fields from the laser and external cavities, and E_c^r and E_e^r are the reflected fields into the cavities.

The terms in this matrix correspond to those of eqn. 8 in Reference 35 and can be directly substituted into this earlier TLLM. The definition of the electric fields is arbitrary. Many works use the root of intensity as a definition. Previous TLLMs have equated the field to the power P of a plane wave confined totally within the active region of width w and depth, d giving

$$|E|^2 = Z_p P/(wd) \quad (2)$$

Z_p is defined as the transverse wave impedance of the guide. However, it is difficult to use this description at interfaces, unless one assumes that the wave will be similarly confined outside the cavity. A more useful definition is to use normalised fields, so that they are proportional to the square root of the optical wave powers in the respective regions:

$$|E|^2 = kP \quad (3)$$

where k is a constant. This allows the matrix of eqn. 1 to be defined for a butt interface between a laser cavity with index n_1 and an external cavity with index n_2 as [22, 23]

$$S_{11} = -S_{22} = (n_1 - n_2)/(n_1 + n_2) \quad (4)$$

$$S_{12} = S_{21} = 2\sqrt{(n_1 n_2)}/(n_1 + n_2) \quad (5)$$

These terms do not have any frequency dependence in this model. However, they can be used to describe short (a few wavelengths) intercavity couplers, whose frequency dependence is negligible over the lasing bandwidth. Their values are given in References 22, 23 and 40. Note that the only consequence of this scaling is to simply scale the field in the external cavity.

For a simple plane mirror nondispersive cavity reflector, the cavity is simply a software delay, i.e.

$$E_e^i(t + T) = R_3 \cdot E_e^r(t) \quad (6)$$

where t is an integer number of timesteps, T is the round-trip delay of the external cavity, and R_3 is the field reflectivity of the mirror multiplied by any propogation losses incurred during a round trip in the external cavity. Note that it is convenient to use a delay of an integer number of timesteps, m, so that the returning samples are in step with the samples in the laser cavity model. The external cavity's delay is thus related to the sampling timestep, ΔT, by

$$T = m\,\Delta T \quad (7)$$

The delay can be thought of as a cavity of $m/2$ sections in length, noting that each section stores both outward and returning wave samples to give a delay equal to m timesteps. The sampling timestep defines the optical bandwidth in the model and also the number of modelling sections s along the laser chip. Interestingly, the modelled bandwidth, in longitudinal modes, is equal to s. Usually s is chosen to be between 10 and 100, the upper limit being set by the available computing resources.

An alternative to using an integer number of timesteps delay for the external cavity is to use a stub attenuator model, as described in Reference 33. This could be used to alter the effective delay of the cavity over a limited frequency range, without having to use a small sampling interval and, consequently, increasing the computational task.

For dispersive reflector cavities a frequency selective model must be included within the delay. A simple model would be an *RLC* bandpass filter as used to represent stimulated emission in the TLLM [32]. This would have a Lorentzian response, whose peak could be matched to the peak of the grating response. Alternatively, if a short enough sampling interval were to be used, a grating or multilayer filter could be represented by a digital filter. This paper will concentrate on cavities without dispersive reflectors.

4 Short external cavity simulations

A device consisting of a short-cavity Fabry-Perot laser coupled to a graded-index rod (GRINrod) lens is used as an example. The GRINrod was assumed to be butted against the rear facet of the laser, with no airgap. The outer end of the GRINrod was assumed to be uncoated, giving a field reflectivity (including propagation losses) of 0.29. The scattering losses, refractive indices, and approximate device dimensions were taken from Reference 24. The material parameters, for a 1540 nm device, are from Reference 41.

The use of a short laser cavity and a short external cavity should give high relaxation frequencies, similar to the short-coupled cavity (SCC) laser suggested in References 7 and 8. The device parameters are given in Table 1.

Table 1: Laser parameters

Symbol	Parameter name	Value	Unit
λ_0	gain-peak wavelength	1538.65	nm
L	laser cavity length	200	μm
L'	external cavity length (Figs. 2–8)	166.7	μm
L'	external cavity length (Fig. 9)	4.0	cm
w	active region width	2.00	μm
d	active region depth	0.15	μm
Γ	optical confinement factor	0.4	
$\bar{n}_e$	laser cavity group index	4.0	
$\bar{n}_e$	external cavity group index	1.5	
n_1	laser cavity erfective index	3.5	
n_2	external cavity effective index	1.5	
N_0	transparency carrier density	0.9×10^{18}	cm^{-3}
a	laser gain constant	2.7×10^{-16}	cm^2
α_{sc}	laser scattering attenuation	30	cm^{-1}
R_1	front facet power reflectivity	0.3	
τ_s	carrier lifetime	2.0	ns
c	vacuum velocity of light	3×10^{10}	cm/s

A model with 32 sections for the laser and 10 sections for the resonator was used. These values give a beating period between the laser and resonator modes of 16 laser modes. An even number of resonator sections ensures that the dominant mode lies at the centre of the modelled bandwidth. This bandwidth is offset from zero frequency by

$$f(\text{offset}) = b/\Delta T \quad (8)$$

Where b is an arbitrary integer and ΔT is the timestep.

This gives a frequency offset of 192 THz for the parameters in Table 2.

Table 2: Model parameters

Symbol	Parameter name	Value
s	number of laser cavity sections	32
s'	number of external cavity sections	10/2400
b	model bandnumber	16
ΔT	iteration timestep	8.3333×10^{-14} s
S_{11}	laser-laser cavity field reflectivity	0.4
S_{21}	laser-external cavity transmittance	0.9165
S_{22}	external-external cavity reflectivity	−0.4
S_{12}	external-laser cavity transmittance	0.9165
R_3	external mirror field reflectivity including cavity losses	0.29
Q	gain curve model Q-factor	12

The timestep is constrained by the laser group velocity, cavity length and number of model sections; thus the dominant resonance frequency is not a free parameter [32]. However, in practice, the offset frequency is arbitrary, because the only error introduced by making b noninteger is to slightly alter the width of the gain curve, and this can be compensated for. Note that the gain peak has been fixed at the centre of the modelled bandwidth to correspond to the dominant resonance.

3.1 Threshold gain and carrier density

The threshold gain for external cavity lasers may be obtained by replacing the rear facet and cavity system with an effective mirror with a complex wavelength-dependent field reflectivity [40]:

$$R_e = S_{11} + \frac{S_{12} S_{21} R_3}{1 - S_{22} R_3} \tag{9}$$

Where R_3 is the reflectivity of the external mirror system including the propagation losses and phase shifts to and from the laser facet. The value of R_3 for the dominant mode (R maximised near to the gain curve peak) can be substituted into the steady state solutions of the rate equations to obtain the threshold gain and carrier density [42].

The threshold gain can be obtained from the TLLM by modelling a switch-on transient and noting the carrier density after the transient has settled. The dominant mode may then be identified by taking a Fourier transform of the sampled optical field after the transient has settled.

A transient response to a step increase in injection current to 80 mA was used to check whether the carrier density settled to the threshold value calculated for the dominant mode. This high current was used to ensure that the model quickly reached a steady state. The threshold carrier density was found to be $(1.663 \pm 0.02) \times 10^{18}$ cm^{-3}.

A Fourier transform of the last 1024 iterations revealed that the spectrum settled to the central dominant mode with the side modes at less than −22 dB. At this frequency, the value of R_l is at a maximum (0.618). The theoretical threshold carrier density is therefore 1.680×10^{18} cm^{-3}. The calculated threshold current is 8.07 mA.

The difference between theoretical and experimental threshold carrier densities is probably a result of the assumption that the spontaneous emission is zero in the theoretical calculation (i.e. the round-trip gain is assumed to be equal to the loss), whereas it is included in the numerical simulation (i.e. the gain plus the spontaneous emission equals the loss). This gives a slightly lower carrier density in the numerical simulation.

3.2 Transient response excluding laser chirp

The TLLM was used to compare the evolution of spectra from external cavity and Fabry-Perot devices. The first comparison assumed that the refractive index in the laser cavity was independent of carrier concentration. All the simulations were for a step increase in injection current from 90% of threshold to 300% of threshold. The spontaneous emission coupling factor to each laser cavity mode was set to 0.00033, equivalent to a factor of 0.001 for each external cavity mode [24].

The transient variations in output power, averaged over 5.3 ps to filter out spontaneous emission noise, and the average carrier concentration, for an external cavity laser are shown in Fig. 2. This shows a classic damped relaxation oscillation [42].

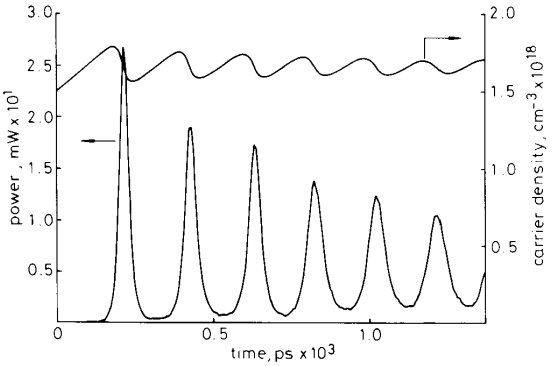

Fig. 2 *Temporal power response and carrier density of an external cavity laser subject to a step increase in injection current to three times theshold*

Linewidth enhancement factor = zero

Figs. 3*a–d* show Fourier transforms associated with the response in Fig. 2, taken over intervals of 85 ps. The first transform (0–85 ps) is dominated by spontaneous emission, which peaks at the laser cavity modes, as expected [43]. The second (85–170 ps) shows more differentiation between the power in the laser cavity modes away from the external cavity modes, and those close to the external cavity modes. In particular, the dominant laser cavity mode coincides with an external cavity mode, as predicted in, for example, Reference 1. The third transform (170–255 ps) shows multimoded lasing indicated by a much larger power spectral density (PSD) and narrower linewidths. Note that only modes close to external cavity modes have lased. Again, the dominant mode lies on an external cavity mode. Fig. 3*d* is a transform taken over the last relaxation pulse in Fig. 2. This shows a side mode suppression of greater than −18 dB.

Fig. 4 is the transient response, an identical device except that the external cavity has been removed. The rear facet power reflectivity was 0.3822, to give identical threshold and photon lifetime characteristics as the external cavity laser. This is equivalent to using an effective mirror model of an external cavity device [40]. When compared with Fig. 2, one outstanding feature is the increased damping rate of the transient. This agrees with experimental observations [44]. The output also appears to be more noisy, possibly owing to beating between the longitudinal modes.

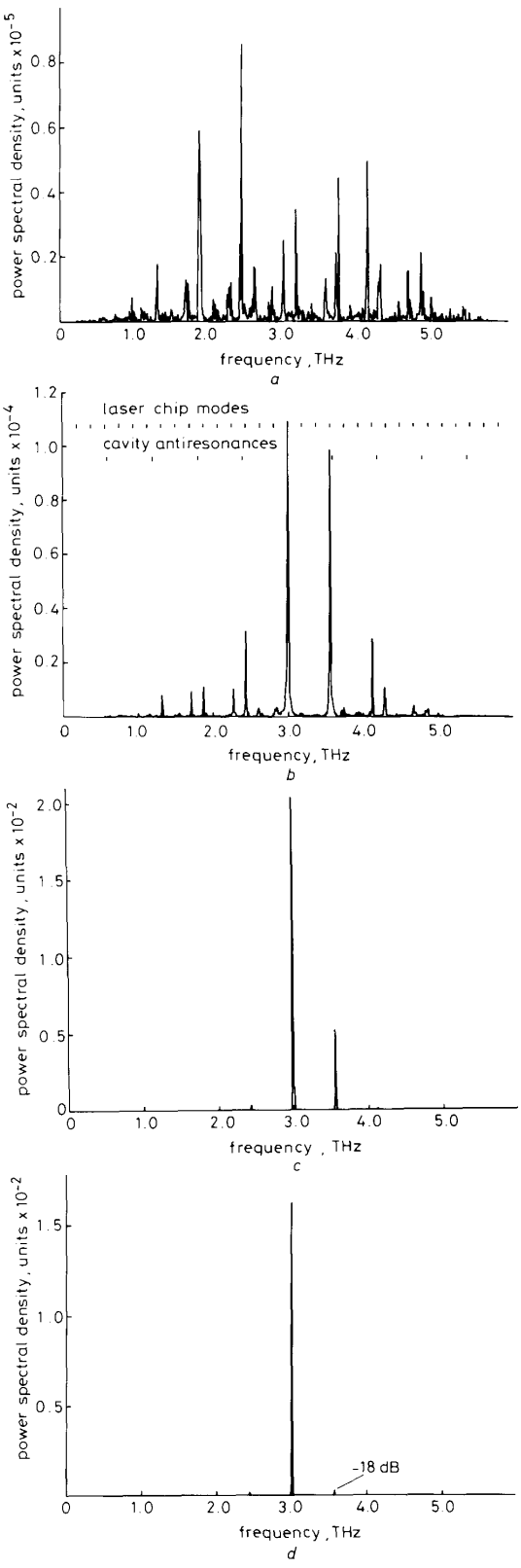

Fig. 3 *Evolution of spectrum corresponding to power response in Fig. 2*
a First 85 ps *b* Second 85 ps *c* Third 85 ps *d* Final optical pulse
Note that the laser oscillates on an antiresonance of the external cavity

Figs. 5*a–d* show spectra from the response of Fig. 4. The first transform (0–85 ps) is very similar to that in

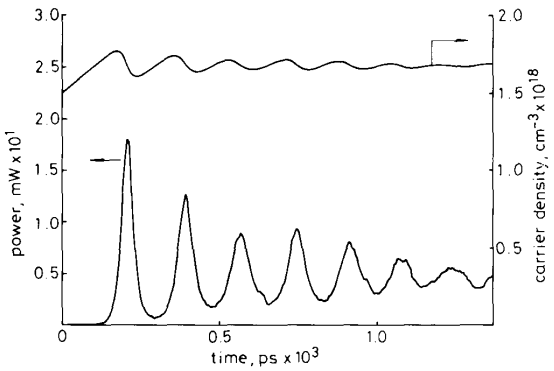

Fig. 4 *Temporal power response of a Fabry-Perot laser subject to a step increase in injection current to three times threshold*
Linewidth enhancement factor = zero

Fig. 3*a*: it is dominated by spontaneous emission into the laser cavity modes. The second transform, however, shows that the only mode selection mechanism in a Fabry-Perot laser is the gain's spectral dependence. The third transform (170–255 ps) shows multimoded lasing. Note that the dominant mode is not at the gain's spectral peak. This is because the random nature of the spontaneous emission has fed more power into one mode below the peak. This randomness would cause mode hopping over a number of pulses. The fourth transform was taken at the end of the transient. The spectrum is much more multimoded than the equivalent external cavity case and the position of the dominant mode would be unpredictable over a number of modulation pulses. These comparisons compare favourably to experimental results for modulated devices [5, 7, 8, 10, 11, 17, 18], and show the single-mode nature of the external cavity laser.

3.3 Transient response including laser chirp

For the second comparison, the index dependence on carrier concentration was included in the model. This has been shown to cause dynamic wavelength shifting of the laser cavity modes inversely proportional to the relaxation power pulse width [33]. However, this shifting has been observed to be smaller in external cavity devices when the dominant Fabry-Perot resonance is detuned (lowered in frequency) from the resonance of the external cavity [45]. This reduction in chirp has also been predicted theoretically [29, 30].

Fig. 6 shows the transient response of an external cavity laser with an index dependence on carrier concentration of -1.85×10^{-20} cm^3. This corresponds to a linewidth enhancement factor also known as Henry's α factor, of 5.6 [41]. The shift in index was set to zero at the threshold carrier concentration so that the dominant mode should be at the centre of the modelled spectrum in the steady state, i.e. zero detuning. The transient response was similar to that in Fig. 2 with a FWHM pulse width of 34 ps for the first pulse.

Figs. 7*a–c* show the associated transforms. The transforms were taken over 2048 iterations (170 ps) to improve the spectral resolution and so that the whole of the first relaxation pulse was included in the second transform. This shows the 'rabbit-ear' spectrum of a single mode, as described in Reference 33. The spectral width Δf of this

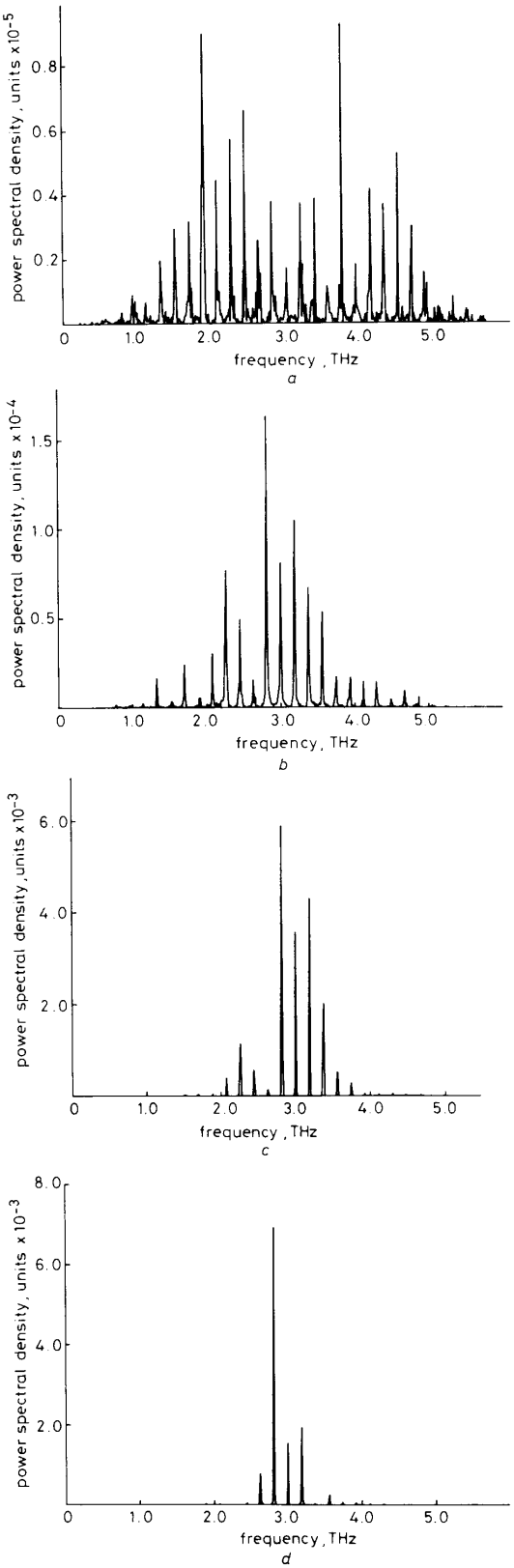

Fig. 5 *Evolution of spectrum corresponding to power response in Fig. 4*
a First 85 ps *b* Second 85 ps *c* Third 85 ps *d* Final optical pulse

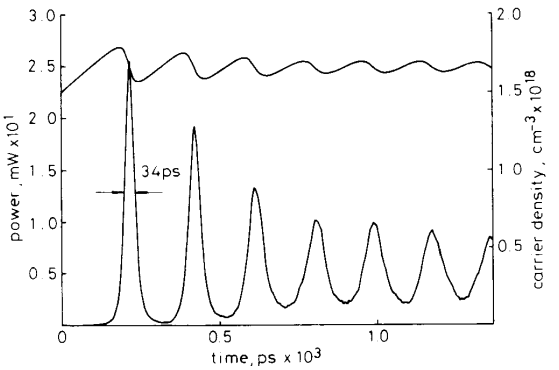

Fig. 6 *Temporal power response of external cavity laser subject to a step increase in injection current to three times threshold.*
Linewidth enhancement factor = 5.6

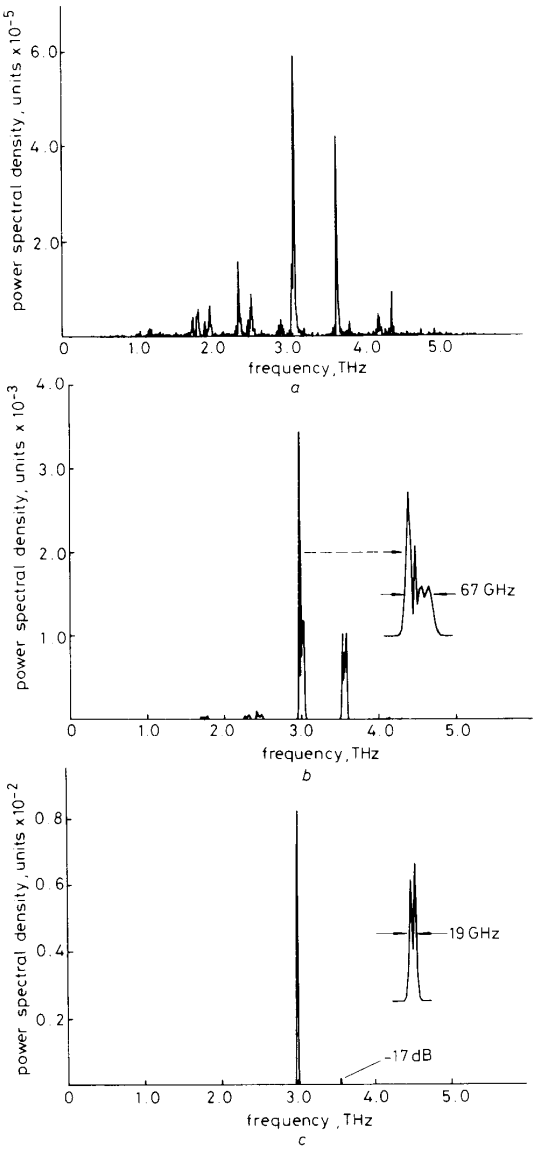

Fig. 7 *Evolution of spectrum corresponding to power response in Fig. 6*
a First 170 ps *b* Second 170 ps *c* Final optical pulse

ear is 67 GHz. The final transform shows a side-mode suppression of more than −17 dB, comparable with the unchirped simulations.

If Gaussian pulses and spectra are assumed, then the following formula relates the spectral width (FWHM) to the pulsewidth (FWHM):

$$\Delta f \Delta t = 0.441\sqrt{(1 + \alpha^2)} \doteq 2.5 \quad (10)$$

This has been shown to be reasonably accurate for 'rabbit-ear' spectra [33]. For this example, Δf is theoretically 73 GHz. Because of the limited accuracy of the transform (6 GHz resolution) it cannot be said that any chirp reduction has taken place.

To increase the detuning to 10% of the Fabry-Perot free-spectral range, the carrier density for zero chirp was increased to 1.717×10^{18} cm^{-3}. The spectrum of the first pulse showed a decrease in width to 58 GHz (Fig. 8) and a shift towards longer wavelengths. The pulse width remained constant, indicating that a small amount of chirp reduction had occurred. This is less than observed by Dutta *et al.* [45], because of reduced coupling between the cavities, but approximately in agreement with the analytical examples given by Fujita *et al.* [46].

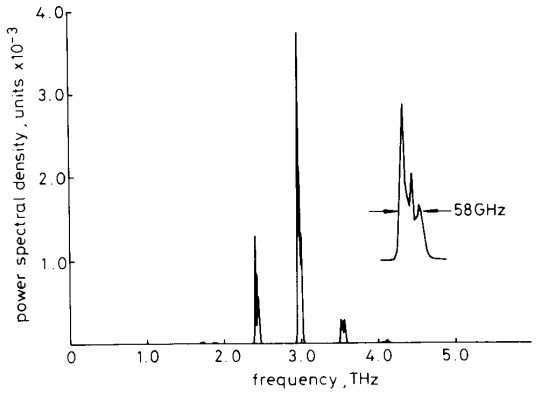

Fig. 8 *Spectrum of first optical pulses when the lasing frequency was detuned by 10% of a chip mode from the feedback resonance*

A further example, with 20% detuning, is shown in Fig. 9*a*. The FWHM of the spectrum was 50 GHz. However, the use of such a large detuning without a dispersive cavity is disadvantageous in the steady state: the spectrum becomes multimoded as other Fabry-Perot resonances move towards external cavity resonances. This is shown in Fig. 9*b*, where the side mode suppression has decreased to −11 dB because of the growth of a long-wavelength side mode. With 30% detuning this side mode became the dominant mode.

5 Long external cavity simulations

A long external cavity is preferable because it should give a narrower linewidth for each mode. However, the cavity modes will be more closely spaced and so a dispersive element may have to be included within the external cavity. Another problem is the delay associated with external cavity: feedback will not take place until the initial pulse has completed a round trip of the external cavity.

The transient response using a 4 cm, 1.5 index cavity with the same losses as the shorter cavity is shown in Fig. 10. A high carrier density is required to initiate the first pulse because the external cavity has yet to provide feedback. The relaxation oscillation is initially similar to that

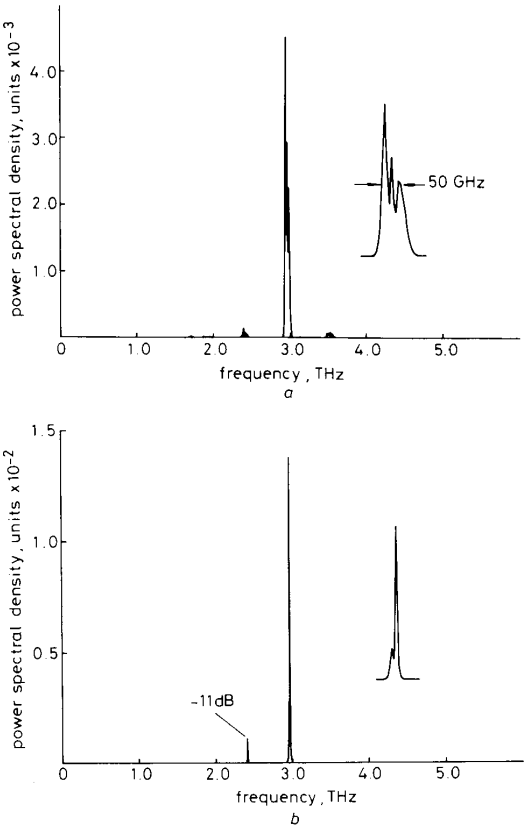

Fig. 9 *Spectra when lasing frequency was detuned by 20% of a chip mode from the feedback resonance*

a First optical pulse
b Final optical pulse

of the short-cavity device, except for a slight increase in threshold carrier density because of the reduced photon lifetime. However, after one round trip, the delayed initial pulse begins to interfere with the response. The response becomes chaotic. This is in contrast to that using rate equations with a delayed term [1], which shows a predictable build-up in power as more power is coupled from the external cavity.

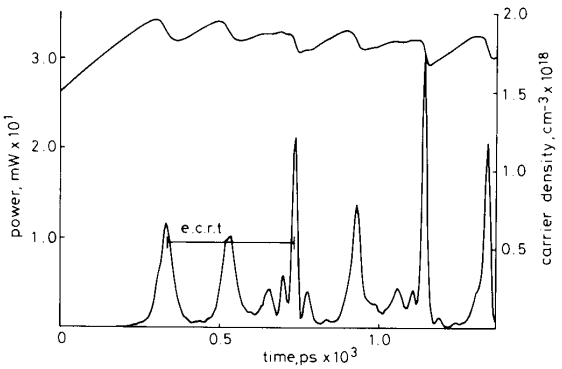

Fig. 10 *Transient response of a long external cavity laser*
The external cavity round-trip (ECRT) time is marked

The spectrum of first complex pulse (middle of Fig. 10) is shown in Fig. 11. This shows multiple laser chip modes

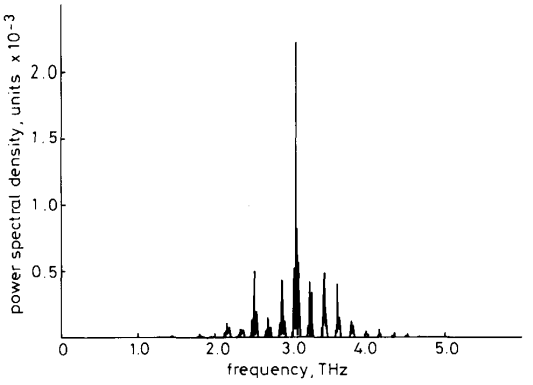

Fig. 11 *Spectrum from middle 170 ps of Fig. 10*
Note the subdivision of the laser chip modes

each partitioned by the external cavity modes which are now closely spaced because of the increased cavity length. A narrowband grating in the external cavity would allow selection of a single laser chip mode and external cavity mode.

The conclusion is that the interference between the spectral components of all the pulses is important, and difficult to predict. However, this interference can produce very narrow pulses. These results also point to the model being useful for mode locked semiconductor lasers, which are simply external cavity devices driven by an RF current at the external cavity's resonance frequency [47].

6 Conclusions

A new model for external cavity lasers has been developed by simple additions to the transmission line laser model. The new model is able to cope with large-signal modulation effects over a wide spectral bandwidth.

Simulations of a short cavity device show single-longitudinal mode (SLM) operation, reduced transient damping and reduced chirp in comparison with a Fabry-Perot device. The detuning between Fabry-Perot and external cavity resonances is critical for chirp reduction, but may cause multimoded behaviour.

The addition of a long cavity to a Fabry-Perot laser has a drastic effect on the device's modulation performance. The use of a model that includes phase shows complex interference patterns in the time and spectral domains. These are not shown by previous models.

Because of the number of parameters that the model can cope with and also the lack of assumptions and approximations, there is almost an infinite number of results to be obtained from the model for a large number of possible device configurations. However, some particularly interesting areas of research include the inclusion of models for gratings, etalons, and interference filters into the external cavity, a more detailed study of the maximum modulation frequency for a given cavity length, the optimisation of feedback to reduce chirp, the propagation of the optical field output along a dispersive fibre, the tunability of external cavity lasers, and the study of unintentional feedback into lasers and laser amplifiers.

7 Acknowledgments

I should like to thank Henning Olesen of the Telecommunication Research Laboratory, Denmark, for interesting discussions during ECOC'88.

8 References

1 SALATHÉ, R.P.: 'Diode lasers coupled to external resonators', *Appl. Phys.*, 1979, **20,** pp. 1–18
2 HENRY, P.S.: 'Lightwave primer', *IEEE J. Quantum Electron.*, 1985, **QE-21,** pp. 1862–1879
3 KLEINMAN, D.A., and KISLIUK, P.P.: 'Discrimination against unwanted orders in the Fabry-Perot resonator', *Bell System Tech. J.*, 1962, **41,** pp. 453–462
4 VAHALA, K., PASLASKI, J., and YARIV, A.: 'Observation of modulation speed enhancement, frequency modulation suppression, and phase noise reduction by detuned loading in a coupled-cavity semiconductor laser', *Appl. Phys. Letts.*, 1985, **46,** pp. 1025–1027
5 PRESTON, K.R., WOOLLARD, K.C., and CAMERON, K.H.: 'External cavity controlled single longitudinal mode laser transmitter module', *Electron. Lett.*, 1981, **17,** (24), pp. 931–933
6 ELISEEV, P.G., ISMAILOV, I., and MANKO, M.A.: 'Injection semiconductor laser with compound resonator', *JEPT Lett.*, 1969, **9,** pp. 362–363 (English Translation)
7 LIN, C., BURRUS, C.A., LINKE, R.A., KAMINOW, I.P., KO, J.S., DENTAI, A.G., LOGAN, R.A., and MILLER, B.I.: 'Short-coupled-cavity (SCC) InGaAsP injection lasers for CW and high-speed single-longitudinal-mode operation', *Electron. Lett.*, 1983, **19,** (15), pp. 561–562
8 LIN, C., BURRUS, C.A., and COLDREN, L.A.: 'Characteristics of single-longitudinal-mode selection in short-coupled-cavity (SCC) injection lasers', *J. Lightwave Technol.*, 1984, **LT-2,** pp. 544–549
9 HAMADA, K., SHIMIZU, H., WADA, M., KUME, M., SHIBUTANI, T., YOSHIKAWA, N., ITOH, K., KANO, G., and TERAMOTO, I.: 'A new monolithic composite-cavity (GaAl)As laser', *IEEE J. Quantum Electron.*, 1986, **QE-22,** pp. 2187–2190
10 STEPHENS, W.E., JOSEPH, T.R., FINDAKLY, T., and CHEN, B.-U.: 'Optical frequency stabilisation of high-power laser diodes under modulation using short optical waveguides', *Electron. Lett.*, 1984, **20,** (10), pp. 424–426
11 LIOU, K.Y.-: 'Single-longitudinal mode operation of injection laser coupled to a grinrod external cavity', *Electron. Lett.*, 1983, **19,** (19), pp. 750–751
12 EDMONDS, H.D., and SMITH, A.W.: 'Second harmonic generation with the GaAs laser', *IEEE J. Quantum Electron.*, 1970, **QE-6,** pp. 356–360
13 FLEMING, M.W., and MOORADIAN, A.: 'Spectral characteristics of external-cavity controlled semiconductor lasers', *IEEE J. Quantum Electron.*, 1981, **QE-17,** pp. 44–59
14 SAITO, S., NILSSON, O., YAMAMOTO, Y.: 'Oscillation centre frequency tuning, quantum fm noise, and direct frequency modulation characteristics in external grating loaded semiconductor lasers', *IEEE J. Quantum Electron.*, 1982, **QE-18,** pp. 961–970
15 WYATT, R., and DEVLIN, W.J.: '10 kHz linewidth 1.5 μm InGaAsP external cavity laser with 55 nm tuning range', *Electron. Lett.*, 1983, **19,** (3), pp. 110–112
16 HO, P.-T.: 'Coherent pulse generation with a GaAlAs laser by active modelocking', *Electron. Lett.*, 1979, **15,** (17), pp. 526–527
17 DUTTA, N.K., GORDON, E.I., SHEN, T.-M., ANTHONY, P.J., and ZYDZIK, G.: 'Single-longitudinal mode operation of a semiconductor laser using a metal film reflection filter', *IEEE J. Quantum Electron.*, 1985, **QE-21,** pp. 559–562
18 HAMMER, J.M., NEIL, C.C., CARLSON, N.W., DUFFY, M.T., and SHAW, J.M.: 'Single-wavelength operation of the hybrid-external Bragg reflector-waveguide laser under dynamic conditions., *Appl. Phys. Letts.*, 1985, **47,** pp. 183–185
19 OLSSON, N.A., HENRY, C.H., KAZARINOV, R.F., LEE, H.J., ORLOWSKY, K.J., JOHNSON, B.H., SCOTTI, R.E., ACKERMAN, D.A., and ANTHONY, P.J.: 'Performance characteristics of a 1.5 μm single-frequency semicondcutor laser with a waveguide Bragg reflector, *IEEE J. Quantum Electron.*, 1988, **24,** pp. 143–147
20 HIROSE, Y., and OGURA, Y.: 'Model for return-beam-induced noise generation in GaAlAs semiconductor lasers', *Electron. Letts.*, 1980, **16,** pp. 202–204
21 MARCUSE, D.: 'Computer model of an injection laser amplifier', *IEEE J. Quantum Electron.*, 1983, **QE-19,** pp. 63–73
22 COLDREN, L.A., and KOCH, T.L.: 'Analysis and design of coupled-cavity lasers — Part 1: Threshold gain analysis and design guidelines', *IEEE J. Quantum Electron.*, 1984, **QE-20,** pp. 659–670
23 COLDREN, L.A., and KOCH, T.L.: 'Analysis and design of

coupled-cavity lasers — Part 2: Transient analysis', *IEEE J. Quantum Electron.*, 1984, **QE-20,** pp. 671–681
24 AGRAWAL, G.P.: 'Generalized rate equations and modulation characteristics of external-cavity semiconductor lasers', *J. Appl. Phys.*, 1984, **56,** pp. 3110–3115
25 TROMBORG, B., OLESEN, H., PAN, X., and SAITO, S.: 'Transmission-line description of optical feedback and injection locking for Fabry-Perot and DFB lasers', *IEEE J. Quantum Electron.*, 1987, **QE-23,** pp. 1875–1889
26 TROMBERG, B., OSMUNDSEN, J.H., and OLESEN, H.: 'Stability analysis for a semiconductor laser in an external cavity', *IEEE J. Quantum Electron.*, 1984, **QE-20,** pp. 1023–1032
27 VAHALA, K., and YARIV, A.: 'Detuned loading in coupled cavity semiconductor lasers — Effect on quantum noise and dynamics', *Appl. Phys. Lett.*, 1984, **45,** pp. 501–503
28 OLESON, H., OSMUNDSEN, J.H., and TROMBERG, B.: 'Nonlinear dynamics and spectral behaviour for an external cavity laser', *IEEE J. Quantum Electron.*, 1986, **QE-22,** pp. 762–733
29 KAZARINOV, R.F., and HENRY, C.H.: 'The relation of line narrowing and chirp reduction resulting from the coupling of a semiconductor laser to a passive resonator', *IEEE J. Quant. Electron.*, 1987, **QE-23,** pp. 1401–1409
30 AGRAWAL, G.P., and HENRY, C.H.: 'Modulation performance of a semiconductor laser coupled to an external high-Q resonator', *IEEE J. Quant. Electron.*, 1988, **QE-24,** pp. 134–142
31 HOEFFER, W.: 'The transmission-line matrix method-theory and applications', *IEEE Trans. on Microwave Theory and Techniques*, 1985, **MTT-33,** pp. 882–893
32 LOWERY, A.J.: 'New dynamic semiconductor laser model based on the transmission-line modelling method', *IEE Proc. J.*, 1987, **134,** (5), pp. 281–289
33 LOWERY, A.J.: 'A model for multimode picosecond dynamic laser chirp based on the transmission line modelling method', *IEE Proc. J*, 1988, **135,** (2), pp. 126–132
34 LOWERY, A.J.: 'A study of the static and multi-Gigabit dynamic effects of gain spectra carrier dependence in semiconductor lasers using a transmission-line laser model', *IEEE J. Quantum Electron.*, 1988, **QE-24,** pp. 2376–2385
35 LOWERY, A.J.: 'A new inline wideband dynamic semiconductor laser amplifier model', *IEE Proc. J*, 1988, **135,** pp. 242–250
36 LOWERY, A.J.: 'A comparison between Fabry-Perot and travelling wave laser amplifiers in an 8 Gbps repeatered optical system using a time-domain model', *J. Phys.D-Applied Physics*, 1988, **21,** pp. S177–S179/ECOOSA88
37 LOWERY, A.J.: 'A new time-domain model for spontaneous emission in semiconductor lasers and its use in predicting their transient response', *Int. J. Numerical Modelling*, 1988, **1,** pp. 153–164
38 LOWERY, A.J.: 'Explanation and modelling of pulse compression and broadening in travelling-wave semiconductor laser amplifiers', *Electron. Lett.*, 1988, **24,** (18), pp. 1125–1126
39 LOWERY, A.J.: 'Transmission-line modelling of semiconductor lasers', May 1988, PhD thesis, Nottingham University
40 COLDREN, L.A., and KOCH, T.L.: 'External-cavity laser design', *IEEE J. Lightwave Technol.*, 1984, **LT-2,** pp. 1045–1051
41 WESTBROOK, L.: 'Measurements of dg/dN and dn/dN and their dependence on photon energy in $\lambda = 1.5$ μm InGaAsP laser diodes', *IEE Proc. J.*, 1986, **133,** (2), pp. 135–142
42 YARIV, A.: 'Optical electronics' (Holt, Rinehart & Wilson, New York, 1985)
43 MARCUSE, D.: 'Classical derivation of the laser rate equation', *IEEE J. Quantum Electron.*, 1983, **QE-19,** pp. 1228–1231
44 RICHE, C., VOUMARD, C., REINHART, F.K., and SALATHE, R.: 'External-cavity-induced non-linearities in the light versus current characteristic of (GaAl)As continuous-wave laser diodes', *IEEE J. Quantum Electron.*, 1977, **QE-13,** pp. 692–696
45 OLSSON, N.A., DUTTA, N.K., and LIOU, K.-Y.: 'Dynamic linewidth of amplitude-modulated single-longitudinal-mode semiconductor lasers operating at 1.5 μm wavelength', *Electron. Lett.*, 1984, **20,** (3), pp. 121–122
46 FUJITA, T., OHYA, J., ISHIZUKA, S., FUJITO, K., and SATO, H.: 'Oscillation frequency shift suppression of semiconductor lasers coupled to external cavity', *Electron. Lett.*, 1984, **20,** (10), pp. 416–417
47 NEW, G.H.C.: 'The generation of ultrashort laser pulses', *Rep. Prog. Phys.*, 1983, **46,** pp. 877–971